IOSR Journal of Applied Physics (IOSR-JAP)
e-ISSN: 2278-4861.Volume 18, Issue 2 Ser. II (Mar – Apr 2026), PP 24-30
www.iosrjournals.org

Spectral, Thermal and Raman Analysis of Tm^{3+} doped in Phosphate Glasses for Optical Temperature Sensor Applications

S.L.Meena
Ceramic Laboratory, Department of physics, Jai Narain Vyas University, Jodhpur 342001(Raj.) India

Abstract
Glass sample of Zinc Lithium Lead Tungsten Alumino Phosphate: (45-x) P_2O_5:10ZnO:10Li_2O:10PbO:10WO_3:15Al_2O_3:xTm_2O_3, (where x=1,1.5 and 2 mol%) have been prepared by melt-quenching technique. The amorphous nature of the prepared glass samples was confirmed by X-ray diffraction. DTA curve was analysed to evaluate the glass transition temperature, crystallization temperature and melting temperature Optical absorption and fluorescence spectra were recorded at room temperature for all glass samples. Judd-Ofelt intensity parameters Ω_λ (λ=2, 4 and 6) are evaluated from the intensities of various absorption bands of optical absorption spectra. Using these intensity parameters various radiative properties like spontaneous emission probability, branching ratio, radiative life time and stimulated emission cross–section of various emission lines have been evaluated

Keywords: *ZLLTAP Glasses, Thermal Properties, Judd-Ofelt Theory, Rare earth ions.*

I. Introduction

Rare-earth doped glasses are technologically important materials as they find applications in lasers, optical devices, optical fiber amplifiers, optoelectronics devices, white light emitting diodes, light converting devices, thermal and mechanical sensors [1-5].The host glass materials should have high refractive index with good chemical and thermal stability. When rare earth ions are added to phosphate glass. They can cause change in the network structure, including the formation of rare earth oxide cluster. These glasses have large values of refractive index, density, dielectric constant and infrared transmittance [6-9]. The addition of Al_2O_3 in to glass can improve the luminescent properties of the material. Phosphate glasses are good materials for investigating laser along with the non-linear uses in optic because of their superior properties such as high refractive index, large phonon energy, low melting temperature, high transparency and thermal stability. Glass ceramics containing thulium oxide have been used high hardness and excellent chemical durability as refractory glasses and band rejection filter[10-15].

The present work reports on the preparation and characterization of rare earth doped heavy metal oxide (HMO) glass systems for lasing materials. I have studied on the absorption and emission properties of Tm^{3+} doped zinc lithium lead tungsten alumino phosphate glasses. The intensities of the transitions for the rare earth ions have been estimated successfully using the Judd-Ofelt theory, The laser parameters such as radiative probabilities(A),branching ratio (β), radiative life time(τ_R) and stimulated emission cross section(σ_p) are evaluated using J.O.intensity parameters(Ω_λ, λ=2,4 and 6).

II. Experimental Techniques

Preparation of glasses

The following Tm^{3+}doped borophosphate glass samples (45-x) P_2O_5:10ZnO:10Li_2O:10 PbO:10WO_3:15Al_2O_3: xTm_2O_3, (where x=1,1.5 and 2 mol%) have been prepared by melt-quenching method. Analytical reagent grade chemical used in the present study consist of P_2O_5, ZnO, Li_2O,PbO,WO_3, Al_2O_3 and Tm_2O_3. They were thoroughly mixed by using an agate pestle mortar. then melted at 965^0C by an electrical muffle furnace for 2h., After complete melting, the melts were quickly poured in to a preheated stainless steel mould and annealed at temperature of 250^0C for 2h to remove thermal strains and stresses. Every time fine powder of cerium oxide was used for polishing the samples. The glass samples so prepared were of good optical quality and were transparent. The chemical compositions of the glasses with the name of samples are summarized in **Table 1.**

Table 1.

Chemical composition of the glasses

Sample	Glass composition (mol %)
ZLLATBP (UD)	45 P_2O_5:10ZnO:10Li_2O:10PbO:10WO_3:15Al_2O_3
ZLLATBP (TM1)	44 P_2O_5:10ZnO:10Li_2O:10PbO:10WO_3:15 Al_2O_3:1Tm_2O_3
ZLLATBP (TM1.5)	43.5 P_2O_5:10ZnO:10Li_2O:10PbO:10WO_3:15 Al_2O_3: 1.5 Tm_2O_3
ZLLATBP (TM2)	43 P_2O_5:10ZnO:10Li_2O:10PbO: 10WO_3:15 Al_2O_3: 2 Tm_2O_3

ZLLATBP (UD) -Represents undoped zinc lithium lead tungsten alumino phosphate glass specimen.
ZLLATBP (TM) -Represents Tm^{3+} doped zinc lithium lead tungsten alumino phosphate glass specimens.

III.Theory

3.1 Oscillator Strength

The intensity of spectral lines are expressed in terms of oscillator strengths using the relation [16].

$$f_{expt.} = 4.318 \times 10^{-9} \int \varepsilon(\nu)\, d\nu \qquad (1)$$

where, ε (*ν)* is molar absorption coefficient at a given energy *ν* (cm^{-1}), to be evaluated from Beer–Lambert law. Under Gaussian Approximation, using Beer–Lambert law, the observed oscillator strengths of the absorption bands have been experimentally calculated [17], using the modified relation:

$$P_m = 4.6 \times 10^{-9} \times \frac{1}{cl} \log \frac{I_0}{I} \times \Delta\upsilon_{1/2} \qquad (2)$$

where c is the molar concentration of the absorbing ion per unit volume, I is the optical path length, $\log I_0/I$ is optical density and $\Delta\upsilon_{1/2}$ is half band width.

3.2. Judd-Ofelt Intensity Parameters

According to Judd [18] and Ofelt [19] theory, independently derived expression for the oscillator strength of the induced forced electric dipole transitions between an initial J manifold $|4f^N (S, L) J\rangle$ level and the terminal J' manifold $|4f^N (S', L') J'\rangle$ is given by:

$$\frac{8\Pi^2 mc\bar{\upsilon}}{3h(2J+1)} \frac{1}{n}\left[\frac{(n^2+2)^2}{9}\right] \times S(J, J') \qquad (3)$$

Where, the line strength S (J, J') is given by the equation

$$S(S', L') = e^2 \sum_{\lambda=2,4,6} \Omega_\lambda \langle 4f^N (S, L)\, J \| U^{(\lambda)} \| 4f^N (S', L')\, J' \rangle^2 \qquad (4)$$

In the above equation m is the mass of an electron, c is the velocity of light, *ν* is the wave number of the transition, h is Planck's constant, n is the refractive index, J and J' are the total angular momentum of the initial and final level respectively, Ω_λ (λ=2,4and 6) are known as Judd-Ofelt intensity parameters.

3.3 Radiative Properties

The Ω_λ parameters obtained using the absorption spectral results have been used to predict radiative properties such as spontaneous emission probability (A) and radiative life time (τ_R), and laser parameters like fluorescence branching ratio (β_R) and stimulated emission cross section (σ_p).

The spontaneous emission probability from initial manifold $|4f^N (S', L') J'\rangle$ to a final manifold $|4f^N (S, L) J\rangle$ is given by:

$$A[(S', L') J'; (S, L) J] = \frac{64\pi^2 \nu^3}{3h(2J'+1)} \left[\frac{n(n^2+2)^2}{9}\right] \times S(J', \bar{J}) \qquad (5)$$

Where, $S(J', J) = e^2 [\Omega_2 \| U^{(2)} \|^2 + \Omega_4 \| U^{(4)} \|^2 + \Omega_6 \| U^{(6)} \|^2]$

The fluorescence branching ratio for the transitions originating from a specific initial manifold $|4f^N (S', L') J'\rangle$ to a final many fold $|4f^N (S, L) J\rangle$ is given by

$$\beta\,[(S', L')\,J'; (S, L)\,J] = \sum_{S\,L\,J} \frac{A[(S' L)]}{A[(S' L')\,J'(\bar{S} L)]} \qquad (6)$$

where, the sum is over all terminal manifolds.

The radiative life time is given by

$$\tau_{rad} = \sum_{S\,L\,J} A[(S', L')\,J'; (S,L)] = A_{Total}^{-1} \qquad (7)$$

where, the sum is over all possible terminal manifolds. The stimulated emission cross -section for a transition from an initial manifold $|4f^N (S', L')\,J'>$ to a final manifold $|4f^N (S, L)\,J>|$ is expressed as

$$\sigma_p(\lambda_p) = \left[\frac{\lambda_p^4}{8\pi c n^2 \Delta\lambda_{eff}}\right] \times A[(S', L')\,J'; (\bar{S}, \bar{L})\bar{J}] \qquad (8)$$

where, λ_p the peak fluorescence wavelength of the emission band and $\Delta\lambda_{eff}$ is the effective fluorescence line width.

IV. Result and Discussion

4.1 XRD Measurement

Figure 1 presents the XRD pattern of the sample contain - P_2O_5 which is show no sharp Bragg's peak, but only a broad diffuse hump around low angle region. This is the clear indication of amorphous nature within the resolution limit of XRD instrument.

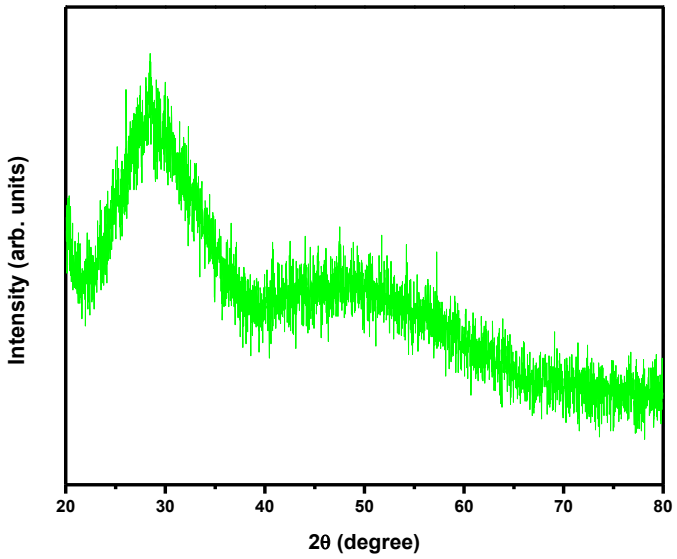

Fig. 1 X-ray diffraction pattern of P_2O_5:ZnO:Li_2O:PbO:WO_3:Al_2O_3:Tm_2O_3.

4.2 Thermal Property

Differential thermal analysis checks the heat absorbed by glass samples during heating or cooling. Fig. 2 depicts the DTA thermogram of powdered ZLLTAP sample. The glass transition temperature (T_g), onset crystallization temperature (T_c), crystallization temperature (T_p), melting temperature(T_m), thermal stability (T_s),Balaji Parameter (B_P), Hurbe's criterion (H_R) and reduced glass transition temperature (T_{rg}) were calculated. Shankar's parameter (K_S) also calculated by using eq. (13). All the determined thermal parameters are given in table 2.

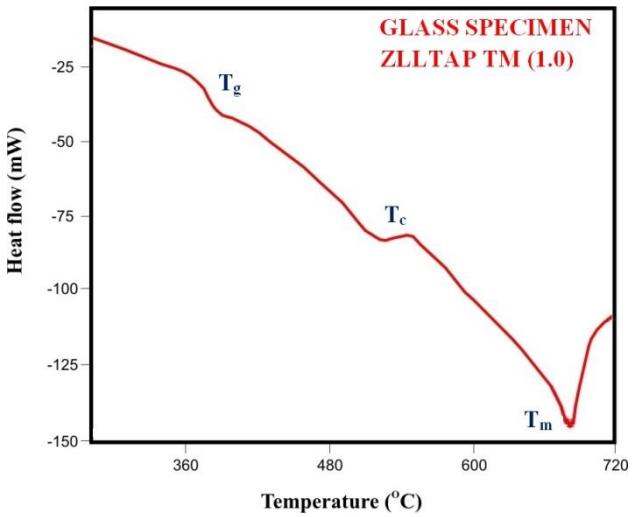

Fig.2: DTA curve of ZLLTAP TM (1.0) glass.

Table 2. Thermal parameters determined from the DTA traces of ZLLTAP TM glasses.

Sample Name	T_g (^{0}C)	T_c(^{0}C)	T_p(^{0}C)	T_m(^{0}C)	T_s(^{0}C)	B_P(^{0}C)	H_R(^{0}C)	K_S(^{0}C)	T_{rg}(^{0}C)
ZLLTAP TM (1.0)	376	510	548	685	134	3.526	0.217	34.234	0.549
ZLLTAP TM (1.5)	380	511	552	687	131	3.195	0.233	33.560	0.553
ZLLTAP TM (2.0)	386	513	556	693	127	2.953	0.239	32.987	0.557

The thermal stability of the glass samples can be calculated by difference between onset crystallization temperature and transition temperature [20].

Thermal stability (T_s) =T_c-T_g (9)

Balaji Parameter can be calculated using [20].

Balaji Parameter (B_P) = [(T_c-T_g)/(T_p-T_c)] (10)

Hruby's criterion is calculated using the Hurby's relation [20].

Hruby's criterion (H_R) = [(T_p-T_c)/(T_m-T_c)] (11)

Reduced glass transition temperature is given as [20].

Reduced glass transition temperature (T_{rg}) =T_g/T_m (12)

Thermal Parameter is given as [20].

K_S= [(T_m-T_c) (T_c-T_g)/T_m] (13)

4.3 Raman Spectra

The Raman Spectrum of zinc lithium lead tungsten alumino phosphate ZLLTAP TM (1.0) glass specimen is recorded and shown in Fig.3.The specimen peaks located at 397 and 775 cm-1.The band 397 cm^{-1} is related to the bending motion of phosphate polyhedral PO_4 units .The broad band at 775 cm^{-1} is due to symmetric stretching of P-O-P bridging oxygen bonds in $(P_2O_7)_4$ units.

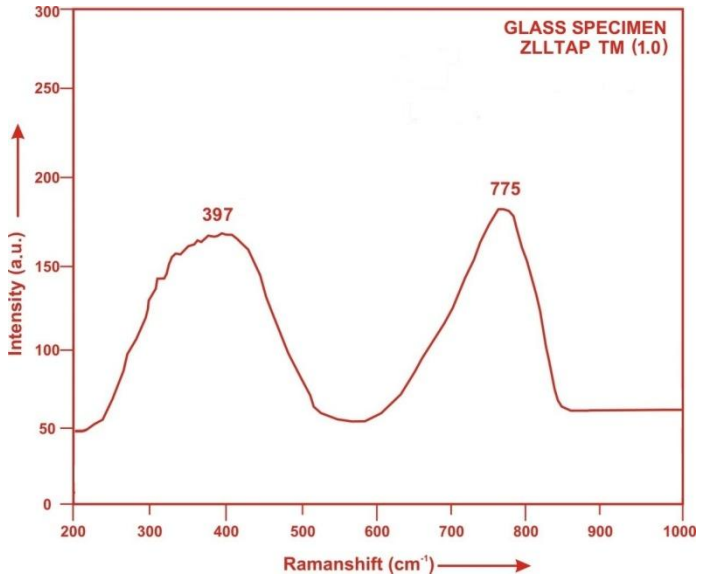

Fig.3: Raman Spectra of ZLLTAP TM (1.0) glass.

4.4 Absorption Spectrum

The absorption spectra of Tm^{3+}doped ZLLTAP glass specimens have been presented in Figure 4 in terms of optical density versus wavelength. Five absorption bands have been observed from the ground state $^3H_6$ to excited states $^3F_4$, $^3H_5$, $^3H_4$, $^3F_3$ and $^1G_4$ for Tm^{3+} doped ZLLTAP glasses.

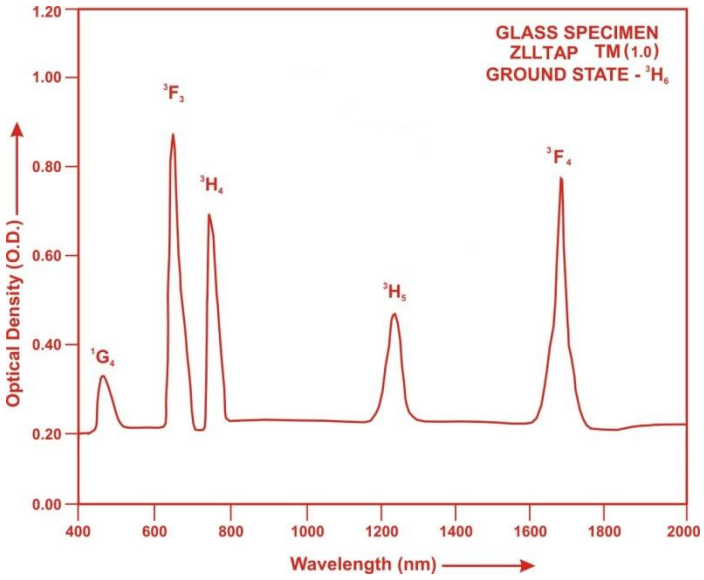

Fig. 4: Absorption spectrum of ZLLTAP TM (1.0) glass.

The experimental and calculated oscillator strength for Tm^{3+} ions in ZLLTAP glasses are given in **Table 3.**

Table 3: Measured and calculated oscillator strength ($P_m \times 10^{+6}$) of Tm^{3+}ions in ZLLTAP glasses.

Energy level from $^3H_6$	Glass ZLLTAP TM(1.0)		Glass ZLLTAP TM(1.5)		Glass ZLLTAP TM(2.0)	
	$P_{exp.}$	$P_{cal.}$	$P_{exp.}$	$P_{cal.}$	$P_{exp.}$	$P_{cal.}$
$^3F_4$	1.86	1.88	1.84	1.86	1.81	1.84
$^3H_5$	1.45	1.44	1.42	1.43	1.40	1.43
$^3H_4$	1.98	2.03	1.95	2.00	1.92	1.99
$^3F_3$	2.98	3.04	2.95	3.01	2.93	3.01
$^1G_4$	0.82	0.88	0.80	0.87	0.77	0.87
r.m.s. deviation	±0.0440		±0.0482		±0.0674	

*Low r.m.s.deviation values clearly indicate the accuracy of fitting.

The values of Judd-Ofelt intensity parameters are given in **Table 4.**

Table 4: Judd-Ofelt intensity parameters for Tm^{3+} doped ZLLTAP glass specimens.

Glass Specimen	$\Omega_2(pm^2)$	$\Omega_4(pm^2)$	$\Omega_6(pm^2)$	Ω_4/Ω_6
ZLLTAP TM (1.0)	6.740	8.989	5.759	1.561
ZLLTAP TM (1.5)	6.607	8.962	5.675	1.579
ZLLTAP TM (2.0)	6.423	8.901	5.688	1.565

4.5. Fluorescence Spectrum

The fluorescence spectrum of Tm^{3+}doped in zinc lithium lead tungsten alumino phosphate glass is shown in Figure 5. There are seven broad bands observed in the Fluorescence spectrum of Tm^{3+}doped zinc lithium lead tungsten alumino phosphate glass. The wavelengths of these bands along with their assignments are given in Table 5. The peak with maximum emission intensity appears at 798 nm and corresponds to the ($^3H_4 \rightarrow {}^3H_6$) transition.

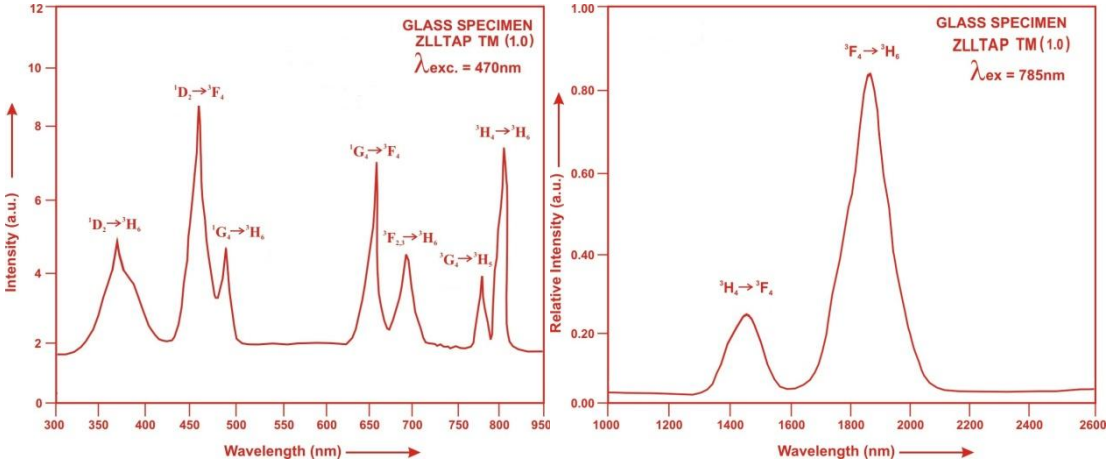

Fig. 5: Fluorescence spectrum of ZLLTAP TM (1.0) glass.

Table5: Emission peak wave lengths (λ_p),radiative transition probability (A_{rad}),branching ratio (β),stimulated emission cross-section(σ_p) and radiative life time(τ_R) for various transitions in Tm^{3+} doped ZLLTAP glasses

Transition		ZLLTAP TM (1.0)				ZLLTAP TM(1.5)				ZLLTAP TM (2.0)			
	λ_{max} (nm)	$A_{rad}(s^{-1})$	β	σ_p (10^{-20} cm^2)	$\tau_R(\mu s)$	$A_{rad}(s^{-1})$	β	σ_p (10^{-20} cm^2)	τ_R (μs)	$A_{rad}(s^{-1})$	β	σ_p (10^{-20} cm^2)	τ_R (10^{-20} cm^2)
$^1D_2 \rightarrow {}^3H_6$	365	53443.50	0.6377	1.510		53205.50	0.6396	1.516		53092.50	0.6421	1.547	
$^1D_2 \rightarrow {}^3F_4$	455	16685.70	0.1991	2.206		16441.60	0.1976	2.212		1609.15	0.1946	2.219	
$^1G_4 \rightarrow {}^3H_6$	480	2188.49	0.0261	0.527		2173.46	0.0261	0.543		2150.70	0.0260	0.570	
$^1G_4 \rightarrow {}^3F_4$	651	702.27	0.0084	1.288	11.9324	695.88	0.0084	1.391	12.0204	696.94	0.0084	1.531	12.0931
$^3F_{2,3} \rightarrow {}^3H_6$	689	5336.86	0.0637	2.277		5292.32	0.0636	2.318		5297.25	0.0641	2.354	
$^1G_4 \rightarrow {}^3H_5$	785	1997.79	0.0238	2.354		1971.49	0.0237	2.412		1971.70	0.0238	2.491	
$^3H_4 \rightarrow {}^3H_6$	798	2666.01	0.0318	4.109		2633.79	0.0317	4.252		2620.12	0.0317	4.367	
$^3H_4 \rightarrow {}^3F_4$	1450	344.74	0.0041	3.645		341.36	0.0041	3.676		338.94	0.0041	3.701	
$^3F_4 \rightarrow {}^3H_6$	1810	439.82	0.0052	7.121		436.44	0.0052	7.146		431.95	0.0052	7.153	

V. Conclusion

In the present study, the glass samples of composition (45-x) ZP_2O_5:10ZnO:10Li_2O:10PbO:10WO_3:15Al_2O_3:xTm_2O_3 (where x =1, 1.5 and 2mol %) have been prepared by melt-quenching method. The value of stimulated emission cross-section (σ_p) is found to be maximum for the transition ($^3H_4 \rightarrow {}^3H_6$) for glass ZLLTAP TM(2.0), suggesting that glass ZLLTAP TM(2.0) is better compared to the other two glass systems ZLLTAP TM(1.0) and ZLLTAP TM(1.5). The high values of Balaji parameter indicate a good thermal stability, therefore these glass samples can find application in fibre fabrication.

References

[1]. Meena,S.L(2025).Spectroscopic and photoluminescence properties of Ho^{3+} doped borate glasses with NIR light emission Applictions,IOSR,Appl.Phys.17,34-40.

[2]. Matos,I.M.,Balzaretti,N.M.(2024).Effect of mixed alkali ions on the structural and spectroscopic properties of Nd^{3+} doped silicate glasses,Res.Mat.21,100517,1-8.

[3]. Zaman,F.,Rooh,G.,Srisittipokakun,N.S.,Wongdeeying,C.,Kim,H.J.,Kaewkhao,J.(2018).Physical,structural and luminescence investigation of Eu^{3+} doped lithium gadolinium bismuth borate glasses for LEDs,Solid State Sci.18,30150.

[4]. Liao,X.,Jiang,X.,Yang,Q.,Wang,L.,Chen,D.(2017).Spectral properties of Er^{3+}/Tm^{3+} co-doped ZBLAN glasses and fibers,Mat.10.486,1-9.

[5]. Meena,S.L.(2025). Spectral, Thermal and Raman analysis of Dy^{3+} doped Borosilicate glasses with large thermal stability parameter, IOSR, Appl.Phys.14,11-18.

[6]. Reddy,M. S.,Uchil, J. and Reddy, C. N. (2014).Thermal and Optical properties of Sodium-Phospho- Zinc-Neodymium oxide glass system, J. of Adv. Sci. Research, 5(2), 32-39.

[7]. Zhang, L., Peng, M.,Dong,G. and Qiua,J.(2012).Spectroscopic properties of Sm^{3+}doped phosphate glasses, J. Mater. Res., 27, 16, 2111-2115.

[8]. Bentouila, O.,Eddine Aiadi, K. Rehouma,F. and Poulain, M.(2013).Spectroscopic studies of rare earth-doped halogeno-phosphate glasses, J. Opt. and Advan. Mat. 15, 11 - 12, 1204-1208.

[9]. Meena,S.L.(2022).Spectroscopic properties of Er^{3+} doped in zinc lithium calcium potassiumniobate phosphate glasses,Int.J.Res.Appl.Sci.Eng.Tech.10,32-37.

[10]. Zhou,Z.Zhou,Y.,Cheng,P.(2017).Effect of B_2O_3 addition on luminescent properties and energy transfer in Er^{3+}/Ho^{3+} codoped tellurite glasses,J.Alloys Comp.717,141-149.

[11]. De,M.,Jana,S.(2020).Optical characterization of Eu^{3+} doped titanium barium lead phosphate glass,Optik-Int.J.for light and Elect.Opt.215,164718,1-7.

[12]. Dhinakarna,A.P.,Vinothkumar,P.,Senthil,T.S.,Kalpana,S.(2024).Investigation on luminescent characteristics of Tb^{3+}/Dy^{3+} co-doped borophosphate glass for cool white LED and radiation shielding applications,Appl.Phys.A,130,709.

[13]. Meena, S.L. (2022). Spectral and FTIR Analysis of Dy^{3+} ions doped Zinc Lithium Cadmium Magnesium Borophosphate Glasses, Int. J. For Res. In App. Sci. and Eng. Technology, 10(8), 55-61.

[14]. Ansari,S.A.,Ansari,M.O.,Alshahrie,A.,Shahadat,M.,Parveen,N.,Darwesh,R.,Aboushoushan,S.F.(2022).Concentration dependent improved spectroscopic characteristics and near white light emission in borophosphate glasses doped with Holmium,Appl.Sci.12,2632,1-15.

[15]. Meena,S.L.(2022).Spectral and Raman analysis of Eu^{3+} doped in zinc lithium cadmium magnesium borophosphate glasses,IOSR,Appl.Phys.14,39-44.

[16]. Meena,S.L.(2025).Spectral and Raman Analysis of Tb^{3+} doped Yttrium Zinc Lithium Ceasium Barium Borate Glasses, IOSR Appl.Phys.17,41-47.

[17]. Meena,S.L.(2021). Spectral and Raman Analysis of Er^{3+} doped Zinc Lithium Antimony Sodalime Tellurite Glasses, Int.J.Eng.Sci.Inv.10, 09-15.

[18]. Judd, B.R. (1962). Optical Absorption Intensities of Rare Earth Ions. Physical Review, 127, 750.

[19]. Ofelt, G.S. (1962). Intensities of Crystal Spectra of Rare Earth Ions. The J. Chem. Phys., 37, 511. [20].Meena,S.L.(2026). Structural, Thermal and Photoluminescence analysis of Pr^{3+} doped borophosphate glasses for the visible light emitting diodes applications, IOSR Appl.Phys.18,55-62.